CHARACTERIZING THE OPERATION OF A ROTATING WALL DEVICE ON A NON-NEUTRAL ION PLASMA

Daniel Erickson

A senior thesis submitted to the faculty of
Brigham Young University
in partial fulfillment of the requirements for the degree of

Bachelor of Science

Bryan Peterson, Advisor

Department of Physics and Astronomy

Brigham Young University

December 2010

Copyright © 2010 Daniel Erickson

All Rights Reserved

ABSTRACT

CHARACTERIZING THE OPERATION OF A ROTATING WALL DEVICE ON A NON-NEUTRAL ION PLASMA

Daniel Erickson

Department of Physics and Astronomy

Bachelor of Science

The rotating wall is a technique that creates an asymmetrical electric field that rotates and couples with the plasma, exerting a torque on it to counteract the drag caused by collisions with neutral atoms. Hardware has been constructed and software has been written to operate the rotating wall, and their proper operation has been verified. However, the ions in our trap are being Debye shielded from the rotating wall signal by the presence of electrons. Attempted methods for removing the electrons, as well as future plans for such, are discussed.

Keywords: Non-neutral Plasma, Ion Plasma

ACKNOWLEDGMENTS

I would first like to thank my advisor Dr. Bryan Peterson for his tireless support both in the lab and in helping edit this paper. I also thank everyone else who assisted in the lab, and those whose prior work made my project possible.

Funding and support for this project came from Brigham Young University's College of Physical and Mathematical Sciences, as well the Department of Physics.

Contents

List of Figures

List of Tables

Chapter 1

Introduction

This project is in support of a larger experiment by the Brigham Young University Plasma Physics Group to accurately measure the half-life of singly ionized Beryllium-7. The generally accepted half-life for ^{7}Be is 53.3 days so to measure it we need to be able to confine a plasma for a comparable length of time.

1.1 Why ^{7}Be?

Beryllium-7 is interesting in that it is the lightest isotope of any element that decays exclusively by electron capture. In this process a 1s (or occasionally 2s) electron combines with a proton to become a neutron, and in the case of ^{7}Be the reaction is shown in Eq. 1.1.

$$^7Be + e^- \longrightarrow ^7Li + \nu_e \tag{1.1}$$

Thus it is expected that the probability of a decay event occurring is proportional to the density of electrons near the nucleus. All previous measurements of the half-life of ^{7}Be have been made either while it is in compound with another element, or while it is implanted in some other medium[1]. Table 1 is a list of previous measurements. These measurements

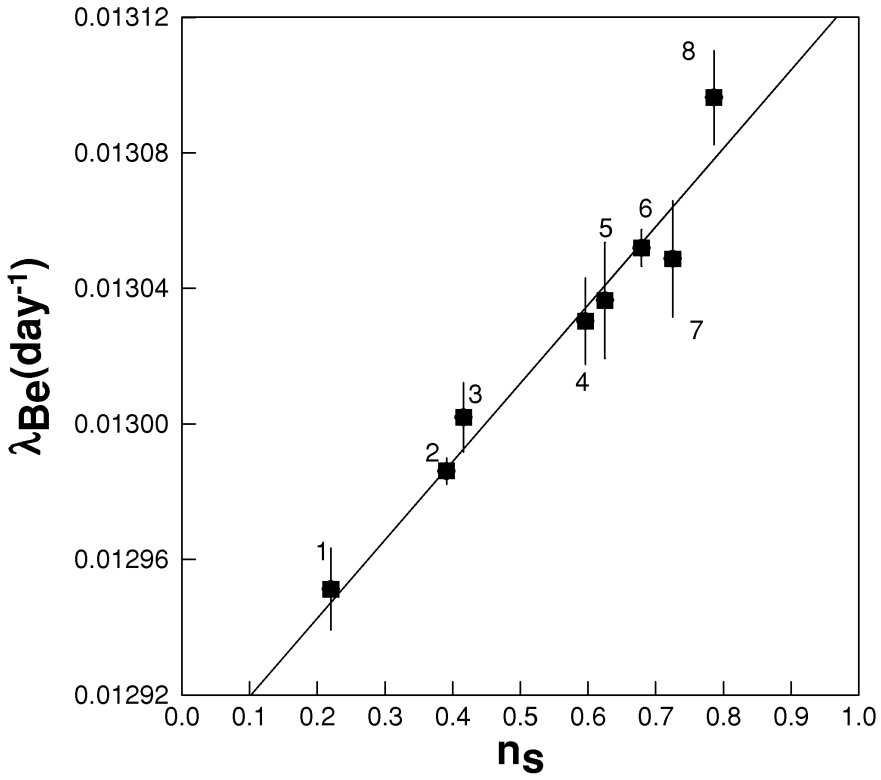

Figure 1.1 Das and Ray's data showing the suggested linear relationship between the decay rate of ^{7}Be and electron density(no. of 2s electrons) near the nucleus.

vary according to the electron affinity of the compound or implant medium.

Das and Ray [1] computed the expected electron density near the nucleus for several compounds and demonstrated a strong positive correlation with a good linear fit. Their results are shown below in Fig. 1.1. Das and Ray suggest that the relationship between the decay rate and the electron density at the nucleus is linear, but acknowledge that their calculated values for electron density may be incorrect. We seek to investigate this claim and establish a baseline value for the half life of ^{7}Be in its singly ionized state.

Table 1.1 Some of the measured values of the half-life of ^{7}Be under varying conditions. The numbers in angle brackets ("<>") indicate the values used in the analysis of P. Das and A. Ray [1].

Environment	$\mathbf{T_{1/2}}$ **(days)**	$\mathbf{\Delta T_{1/2}}$ **(days)**
"Accepted value"	53.22	0.06
BeO [a]	54.226	0.006
$Be^{2+}(OH_2)_4$ [a]	53.694	0.006
BeO, BeF_2, $Be(C_5H_5)_2$ (average) [b] <1>	53.52	0.05
$Be(OH)_2$ [a]	53.416	0.006
$Be(OH)_2$ (gel, p=1 atm) [c]	53.414	0.003
Be [d] <2>	53.376	0.016
Au [e] <3>	53.311	0.042
Be (annealed metal) [f]	53.25	0.04
Ta [e] <4>	53.195	0.052
BN [e]	53.174	0.037
Al [g] <5>	53.17	0.07
Be (annealed metal) [h]	53.12	0.06
LiF [i] <7>	53.12	0.07
Graphite [e] <6>	53.107	0.022
Al_2O_3 [j] <8>	52.927	0.056
$Be(OH)_2$ (gel, p=442 kbar) [c]	52.884	0.022
C_{60} (endohedral) [h]	52.68	0.05
C_{60} (endohedral, T=5 K) [k]	52.47	0.04

[a] Chih-An Huh, Earth Planet. Sci. Lett. **171**, 325-328 (1999).
[b] H. W. Johlige, *et al.*, Phys. Rev. C **2**(5), 1616-1622 (1970).
[c] Lin-gun Liu, Chih-An Huh, Earth Planet Sci Lett. **180**, 163-167 (2000).
[d] Zhi-Yi Liu, *et al.*, Chin. Phys. Lett. **20**(6), 829 (2003).
[e] E. B. Norman, *et al.*, Phys. Lett. B **519**, 15-22 (2001).
[f] T. Ohtsuki, *et al.*, Mater. Trans. **48**(4), 646-648 (2007).
[g] F. Lagoutine, *et al.*, Int. J. Appl. Radiat. Isot. **26**, 131-135 (1975).
[h] T. Ohtsuki, *et al.*, Phys. Rev. Lett. **93**(11), 112501 (2004).
[i] M. Jaeger, *et al.*, Phys. Rev. C **54**(1), 423-424 (1996).
[j] A. Ray, *et al.*, Phys. Lett. B **455**, 69-76 (1999).
[k] T. Ohtsuki, *et al.*, Phys. Rev. Lett. **98**(25), 252501 (2007).

1.2 Why does ^{7}Be matter?

Beryllium-7 is important because it is part of the proton-proton cycle by which the sun fuses hydrogen into helium. The first step in the cycle, shown in Eq. 1.2, is called the pp reaction

$$p + p \longrightarrow {}^2H + e^+ + \nu_e \tag{1.2}$$

and in stars similar to the sun is the source of almost 100% of the deuterium inside it[2]. This reaction is followed quickly by fusion with another proton to form ^{3}He as shown in Eq. 1.3.

$${}^2H + p \longrightarrow {}^3He + \gamma \tag{1.3}$$

At this point the process can proceed along one of four separate branches, but one is so rare in sun-like stars that we will ignore it. The first, Eq. 1.4, involves the fusion of two ^{3}He nuclei to form a ^{4}He nucleus and two free protons,

$${}^3He + {}^3He \longrightarrow \alpha + 2p \tag{1.4}$$

and creates approximately 85% of the ^{4}He in the sun[2]. The second, Eq. 1.5, begins with the fusion of a ^{3}He and a ^{4}He to form ^{7}Be, which later decays to ^{7}Li.

$$\begin{aligned} {}^3He + {}^4He &\longrightarrow {}^7Be + \gamma \\ {}^7Be + e^- &\longrightarrow {}^7Li + \nu_e \\ {}^7Li + p &\longrightarrow 2\alpha \end{aligned} \tag{1.5}$$

The lithium reacts with a free proton to form two ^{4}He nuclei, and helium produced in this way is roughly the remaining 15%[2]. The third path (eq. 1.6) is responsible for only about .02% [2] of ^{4}He produced in the sun, but does involve the production and reaction of ^{7}Be so

it is important as well.

$$\begin{aligned} {}^7Be + p &\longrightarrow {}^8B + \gamma \\ {}^8B &\longrightarrow {}^8Be^* + e^+ + \nu_e \\ {}^8Be^* &\longrightarrow 2\alpha \end{aligned} \tag{1.6}$$

If we can achieve a better understanding of the relationship between the half-life of ^{7}Be and the electron density near its nucleus we will be better able to understand the processes taking place inside the sun, specifically the different rates at which such reactions take place.

Each set of reactions (Eqs. 1.5 and 1.6) releases an electron neutrino, but the neutrinos from these reactions have different energies. At present the ^{7}Be neutrinos can be detected by the Borexino detector at the Laboratori Nazionali del Gran Sasso in Italy[3], and the ^{8}B neutrinos can be detected by the Sudbury Neutrino Observatory in Canada[4], but there does not currently exist a detector capable of observing both. Consequently an accurate measure of the relative incidence rates of these two neutrinos cannot be made. A better understanding of the half life of ^{7}Be will allow us to make better predictions about the rates of occurrence of these two reactions.

Besides being produced in the sun, ^{7}Be is found at high altitudes in the Earth's atmosphere. In 1984 NASA launched the Long Duration Exposure Facility(LDEF) shown in Fig. 1.2, which was a satellite designed to study the effect of long term exposure to the environment of space on various materials[5]. It was stabilized in its motion so that the same end always pointed toward the earth, and the leading edge was also held constant. It was retrieved from orbit approximately six years later, and a gamma ray spectrum revealed that the activity due to ^{7}Be on the leading edge was two orders of magnitude greater than the activity on the trailing edge[5]. This suggests that the ^{7}Be was swept up from the atmosphere, and was not the product of a reaction with the incident radiation. It has been known for many years that ^{7}Be can be produced in the upper atmosphere as the result of a collision

Figure 1.2 NASA's LDEF satellite as seen from orbit. It was used to study the effects of long-term exposure to the environment of space on various materials. Image retrieved from http://www.astronautix.com/graphics/0/10061447.jpg

between high energy cosmic rays and nitrogen or oxygen atoms[6]. The rate at which ^{7}Be is produced in the upper atmosphere is both a function of altitude and latitude, but is fairly well defined. Peak ^{7}Be production occurs at around 20 km altitude[5]. Above that point the rate of production varies with the density of nitrogen and oxygen, and below it the cosmic rays become too attenuated. One of the most perplexing results of the LDEF experiment is that the amount of ^{7}Be found embedded in the plates was three orders of magnitude greater than predicted[5].

In the lower atmosphere the ^{7}Be precipitates with the rain, and since the rate at which it is produced can be predicted with reasonable accuracy, the amount of ^{7}Be present in sediment deposits can be used to trace them through river systems[7].

1.3 Making the measurement

To accurately measure the half-life of ^{7}Be we need to be able to maintain plasma confinement for approximately as long as the half-life. In theory all this requires is providing radial and axial confinement, but in practice collisions with background neutral gas particles exert a drag on the plasma and cause it to expand[8]. Ordinary plasma lifetimes for our system are approximately five minutes. For some experiments it would suffice to replace the plasma as needed, but when measuring the half-life it is important that the same ions remain in the trap so we can accurately determine how many undergo decay. The "rotating wall" is a technique designed to exert a torque on the plasma that counteracts the drag caused by neutral atoms and will allow us to increase the confinement time of our plasma by several decades.

Chapter 2

Our apparatus

2.1 The trap

Our trap is a Malmberg-Penning style trap with a large cylindrical electromagnet producing strong axial magnetic fields (.45 T) and providing radial confinement. The trap itself is evacuated to the 10^{-9} torr range to minimize collisions with neutral atoms. Situated inside the trap is a series of ring shaped electrodes. The end rings are raised to high voltage (+150 V) to provide longitudinal confinement, and the others are used for our various controls and diagnostics. See Fig. 2.1 for a schematic representation of a Malmberg-Penning trap, and Fig. 2.2 for a picture of our electrodes.

Several of the components of our trap are made of either 304 or 316 stainless steel. These materials were chosen specifically for their tendency not to easily magnetize, but like all types of stainless steel they do outgas hydrogen. All other parts inside the vacuum system are made of either oxygen-free high conductivity(OFHC) copper, or aluminum. The hydrogen from the stainless steel comprises the majority of the neutral atoms in our trap, with the rest likely being water vapor.

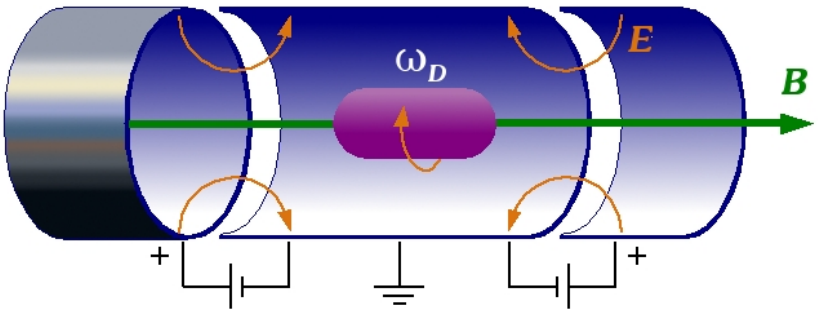

Figure 2.1 Schematic representation of a Malmberg-Penning trap with a grounded confinement region and high end potentials. The plasma rotates with an $E \times B$ drift frequency ω_D.

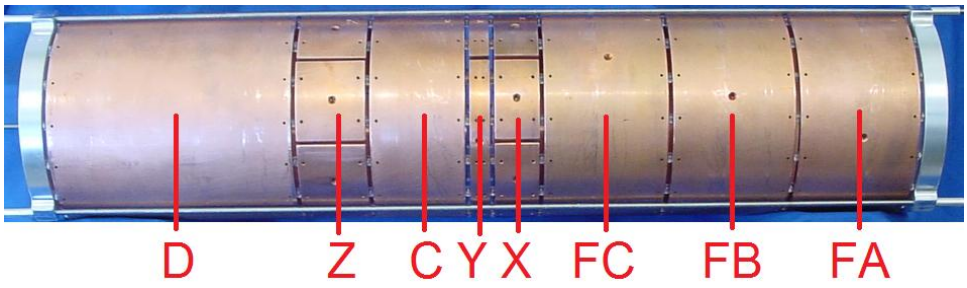

Figure 2.2 Picture of the electrode configuration of our trap.

2.2 Rotating Wall

The "rotating wall" electric field is an asymmetrical field produced by applying a sinusoidal voltage signal to each of eight sectors of a ring that surrounds the plasma. Each sector is phase shifted 45 degrees with respect to those next to it, and the effect is that of a dipole that rotates with the plasma about a common axis. The frequency at which the fields rotate is chosen based on the $E \times B$ frequency of the plasma. Huang defines a "slip" frequency, $\Delta f = f_w - f_e$, as the difference between the drive frequency f_w and the $E \times B$ drift frequency f_e. For the plasma to be compressed it is necessary that $\Delta f > 0$ [9]. It is believed that the rotating wall causes plasma compression by coupling with and exciting plasma modes known as Trivelpiece-Gould modes. These modes then transfer their angular momentum to the plasma via wave-particle coupling mechanisms such as Landau damping[10]. The rotating wall signals in our trap are applied to the ring marked "X" in Fig. 2.2.

To apply the signal to each ring segment we built eight amplifiers of identical gain, four inverting and four non-inverting, whose circuit diagrams are displayed in Figure 2.3. NE5532N op-amps were used because each chip contains two amplifiers, allowing us to minimize the board space required. For a picture of the finished amplifiers see Fig. 2.4. This choice was made to enable us to use just four control lines due to hardware restrictions. For example, the fifth ring segment is to be phase shifted 180 degrees with respect to the first, and so it uses the same signal as the first section, but through an inverting amplifier instead of a non-inverting one. Similarly, the second and sixth rings share a control line, as does the third with the seventh, and the fourth with the eighth. In this configuration the apparatus produces a dipole field, but we can easily alter the phase relationships in our control software and swap a few cables to set up a quadrupole field as well. However, Huang suggests that it is the dipole field that is the most effective because it produces a field that is nonzero at the center of the plasma[9]. Our rotating wall is controlled by two National

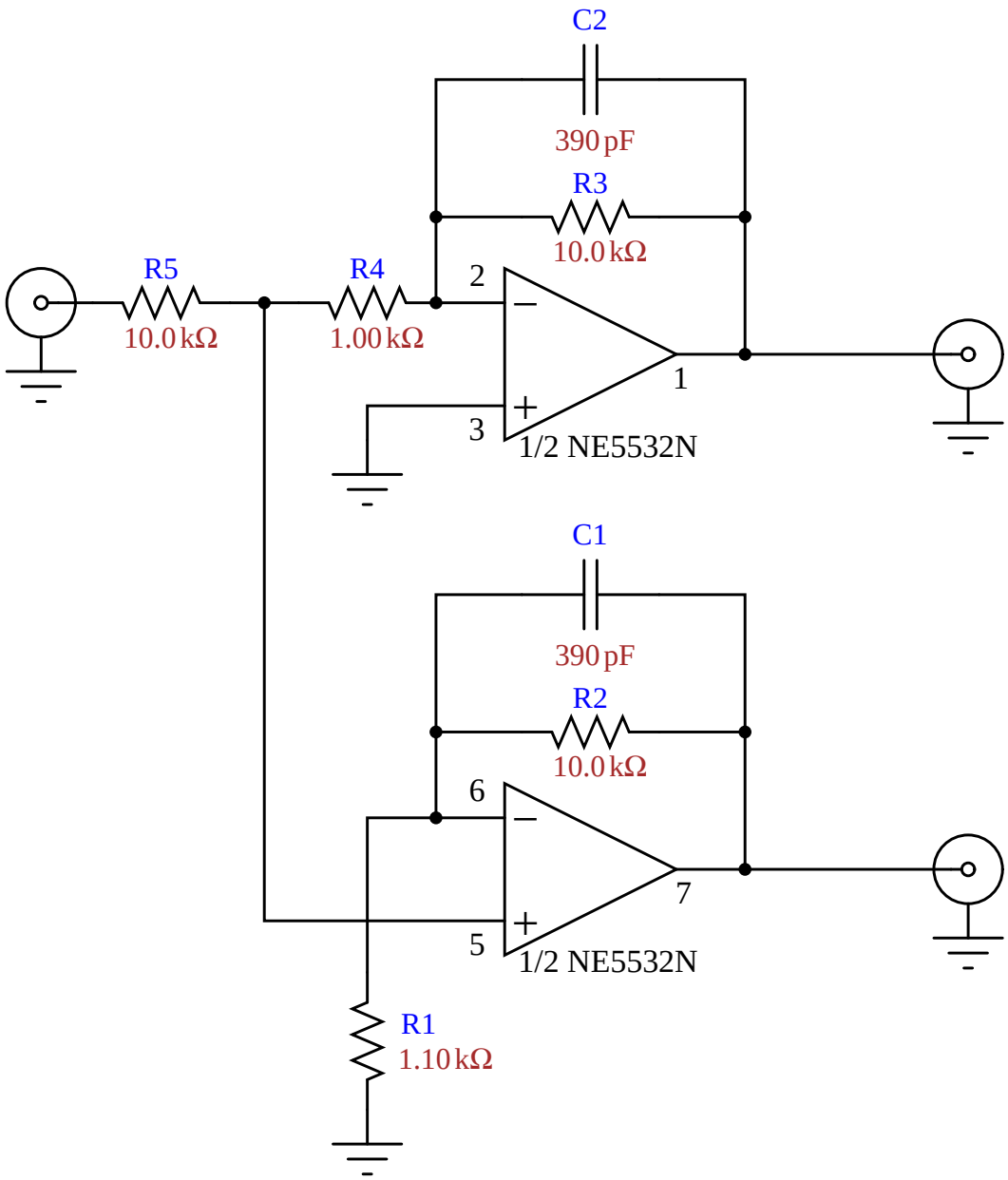

Figure 2.3 Circuit diagrams for the amplifiers used to drive the rotating wall. Four identical sets were produced.

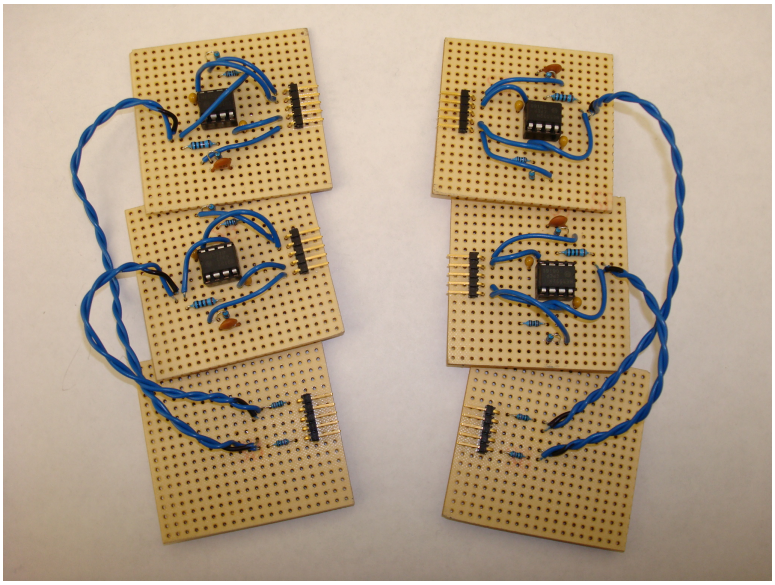

Figure 2.4 The completed amplifiers before installation. Due to limitations of the number of connections available to each board inputs were taken on a separate board and the connections of each amplifier board were reserved for outputs.

Instruments USB-6211 boards which each have two analog output channels. Programming was done in LabVIEW and used two separate VI's. The first creates tasks for each control line and writes out an identical sinusoidal signal to all four. We discovered that the internal clocks of the two boards were not well synchronized, so in order to maintain the proper phase relationship we triggered all our analog signals off of a digital clock signal generated by one of the boards. We also had to incorporate a digital trigger signal from one of the boards to ensure that all the signals started at the same time. The second VI is run just before dumping the plasma and grounds all ring sectors, then clears the tasks from memory. Block diagrams for these VI's are included in Appendix A.

Chapter 3

Testing

3.1 The hardware

To test the amplifiers we hooked each one up to a sinusoidal voltage signal over the range of frequencies at which the amplifiers would be expected to operate (2-10 kHz), and compared the input signal with the output on two channels of a digital oscilloscope. Unity gain was observed for all 8 amplifiers. When the amplifiers were driven by the control software we had written, significant high-frequency noise was observed in the output signal due to the finite bitrate of our D/A converter (25 samples/cycle). To eliminate this noise we added capacitors in parallel with the feedback resistors on our amplifiers to serve as low-pass filters. This successfully reduced the noise to acceptable levels, at the cost of a slight reduction in gain. We were also able to verify the direction of rotation of the dipole by overlaying the signals to adjacent ring sectors on a multi-channel oscilloscope. The rotation was confirmed to be in the same direction as the rotation of our ion plasma.

3.2 Problems

One of our biggest difficulties has been having the rotating wall couple with the plasma. Due to the nature of our modified MEVVA source there are lots of electrons present in the plasma that we have thus far been unable to remove[11]. They become trapped under the confinement rings because these regions represent large potential wells due to the electron's negative charge. There is a trade off involved because if the end potentials are very high the electrons spend more time under those rings instead of sloshing through the ion plasma from end to end, but those same high potentials repel the ions toward the center of the trap so that the ion plasma no longer extends under the rotating wall ring. Slightly lowering those end potentials means extending the length of the ion plasma, but it also results in the electrons spending more time in the rest of the ion plasma. If there are too many electrons in the ion plasma they Debye shield the ions such that the rotating wall has no effect.

3.3 Attempted solutions

We have tried a number of solutions for removing the electrons from the trap, most without success. The first attempted solution was to "pump" the electrons out by manipulating the unique configuration of our confinement rings. On the fill end we employ three rings whose voltage can be raised or lowered independently of the others. Ordinarily this would be used to allow us to trap the plasma from several different MEVVA shots without allowing the plasma to escape. If we designate the rings FA, FB, and FC as in Fig. 2.2, with FA being closest to the source, then the trap sequence starts with rings FA and FB at ground and ring FC high. After the source is fired ring FA is raised to trap the plasma under ring FB, between FA and FC, then FC is lowered to allow the plasma to move into our confinement region, and finally FB and FC are raised together to restore the confinement region (rings

X, Y, C, and Z) to its original size. Rings FA and FB can then be lowered again and the process repeated, stacking as many plasma shots as are necessary to achieve the desired plasma density.

We attempted to implement a similar procedure to pump the electrons out of the trap, this time starting with rings FA, FB, and FC, all raised to +150 V. Ring FB was then lowered to divide the electrons into two separate wells under the FA and FC rings. Ring FA is then lowered to discard the electrons underneath it, and all rings are restored to +150 V so the procedure can be repeated as many times as necessary.

Another attempted solution was to "sweep" the electrons out. This solution also required altering the potentials at which the confinement rings were held, but in an entirely different manner. Depending on their temperature, the electrons take different amounts of time to traverse the length of the trap, and by oscillating the end potential at the same frequency we hoped to impart enough extra energy to those electrons to boost them over the confinement rings and out of the trap. Since not all the electrons had the same energy, we swept the frequency of the oscillation up from 1 Mhz to 3 Mhz, hoping to boost all of the electrons over the course of the procedure. We repeated the process several times so that each electron could receive several boosts if needed.

One final attempted solution was to change the order of our rings so that the plasma would extend under the rotating wall ring without us having to compromise too much by lowering the end potentials. Since each of the rings in our confinement region has a different length, and some are divided into different numbers of sectors this could not be accomplished with software or simple switching of cables. The trap had to be opened, the ring assembly removed entirely, and the physical order of the rings changed. Based on the ring designations shown in Figure 2.2 the new order beginning nearest to the source is FA, FB, FC, Y, X, Z, C, D. In this new configuration ring Z is roughly centered over the ion plasma, and the

plasma extends approximately halfway underneath the X ring.

At present, all attempts to remove the electrons have been ultimately unsuccessful. The next procedure we will attempt in order to remove the electrons will be a new sequence of altering ring voltages that begins with lowering all rings in the confinement region to -150 V, then lowering all the end rings to ground. The ions were initially in a 150 V well, and remain in one after the changes so they do not move. The electrons, however, encounter a large potential hill in the middle of the trap, and should all escape to the ends. The original voltages can then be restored with the end rings at +150 V, and the rings in the confinement region being either grounded or used for their respective diagnostics. Hardware for this procedure is currently being constructed and tested.

3.4 Conclusion

We were able to build the amplifiers to run the rotating wall, and write software to control its operation. The correct operation of the control software and the amplifiers has been verified, but we have not yet succeeded in using the rotating wall to increase the confinement time of our plasma. There still exist too many electrons in the plasma from the MEVVA shots and they are Debye shielding the ions from the effects of the rotating wall. We will not be able to proceed until all these electrons are successfully eliminated.

Bibliography

[1] P. Das and A. Ray, "Terrestrial ^{7}Be decay rate and ^{8}B solar neutrino flux," Phys. Rev. C 71, 025801 (1 February 2005).

[2] J. N. Bahcall. *Neutrino Astrophysics* (Cambridge University Press, 1989) p. 63-67.

[3] Borexino Collaboration, "Direct Measurement of the 7Be Solar Neutrino Flux with 192 Days of Borexino Data," Phys. Rev. Lett. 101, 091302 (29 August 2008).

[4] SNO Collaboration, "Independent Measurement of the Total Active 8B Solar Neutrino Flux Using an Array of 3He Proportional Counters at the Sudbury Neutrino Observatory," Phys. Rev. Lett. 101, 111301 (12 September 2008).

[5] G. J. Fishman, et al., "Observation of 7Be on the surface of LDEF spacecraft," Nature 349, 678-680 (21 February 1991).

[6] James R. Arnold, H. Ali Al-Salih, "Beryllium-7 Produced by Cosmic Rays," Science (New Series) 121(3144), 451-453 (1 April 1955).

[7] Sharon A. Fitzgerald, et al., "Beryllium-7 as a Tracer of Short-Term Sediment Deposition and Resuspension in the Fox River, Wisconsin," Environ. Sci. Technol. 35(2), 300-305 (13 December 2000).

[8] J. H. Malmberg, C. F. Driscoll, "Long-Time Containment of a Pure Electron Plasma," Phys. Rev. Lett. 44(10), 654-657 (10 March 1980).

[9] X.-P. Huang, et al., "Steady-State Confinement of Non-neutral Plasmas by Rotating Electric Fields," Phys. Rev. Lett. 78(5), 875 (3 February 1997).

[10] E. M. Hollmann, F. Anderegg, C. F. Driscoll, "Confinement and manipulation of non-neutral plasmas using rotating wall electric fields," Phys. Plasma 7(7), 2776-2789 (July 2000).

[11] D. K. Olson, "Development of a MEVVA based beryllium-7 plasma source," MS Thesis, Brigham Young University, 2007

Appendix A

VI's for controlling the rotating wall

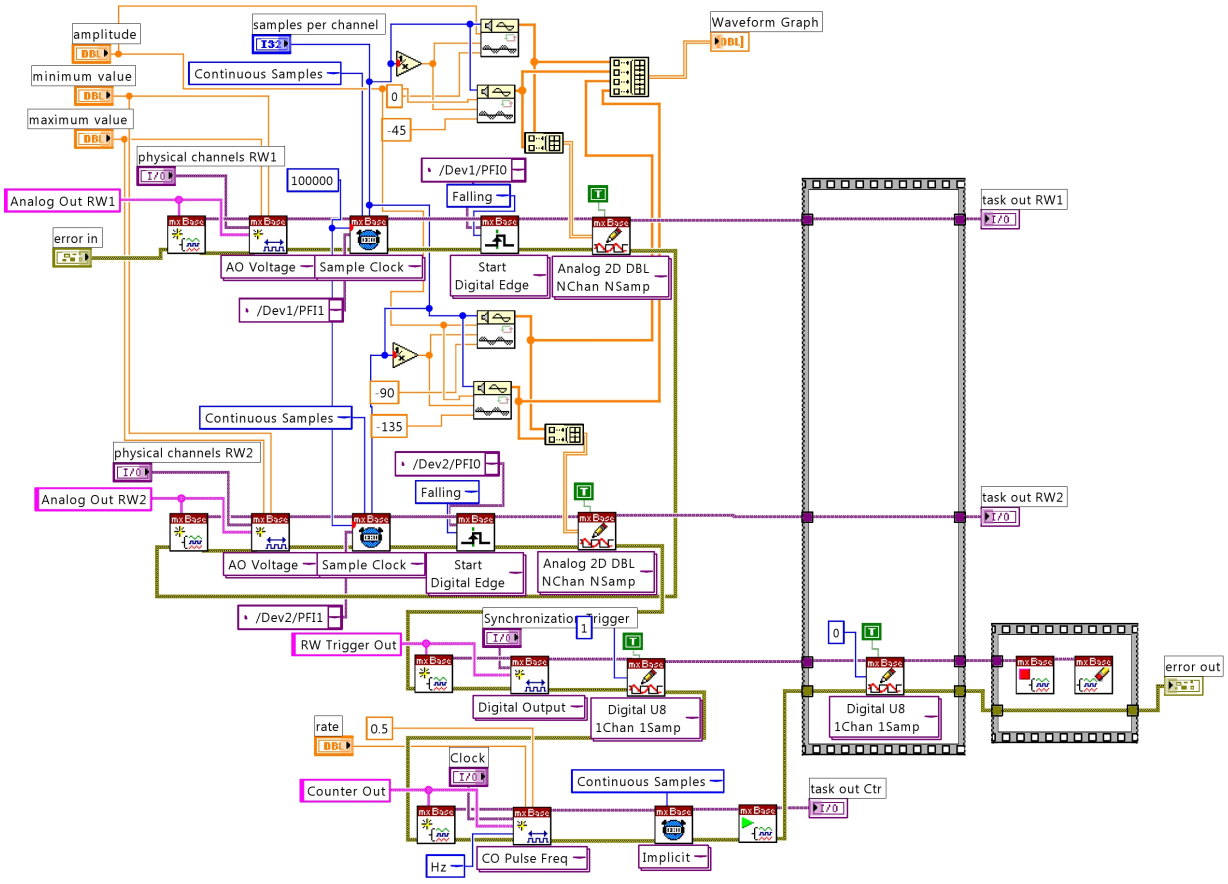

Figure A.1 VI called RWStart used to start the rotating wall, includes external clock and trigger signal. Accepts inputs for all rotating wall parameters such as amplitude and frequency. Two of the outputs are tasks containing the signal for two of the amplifier pairs, and the third is the clock.

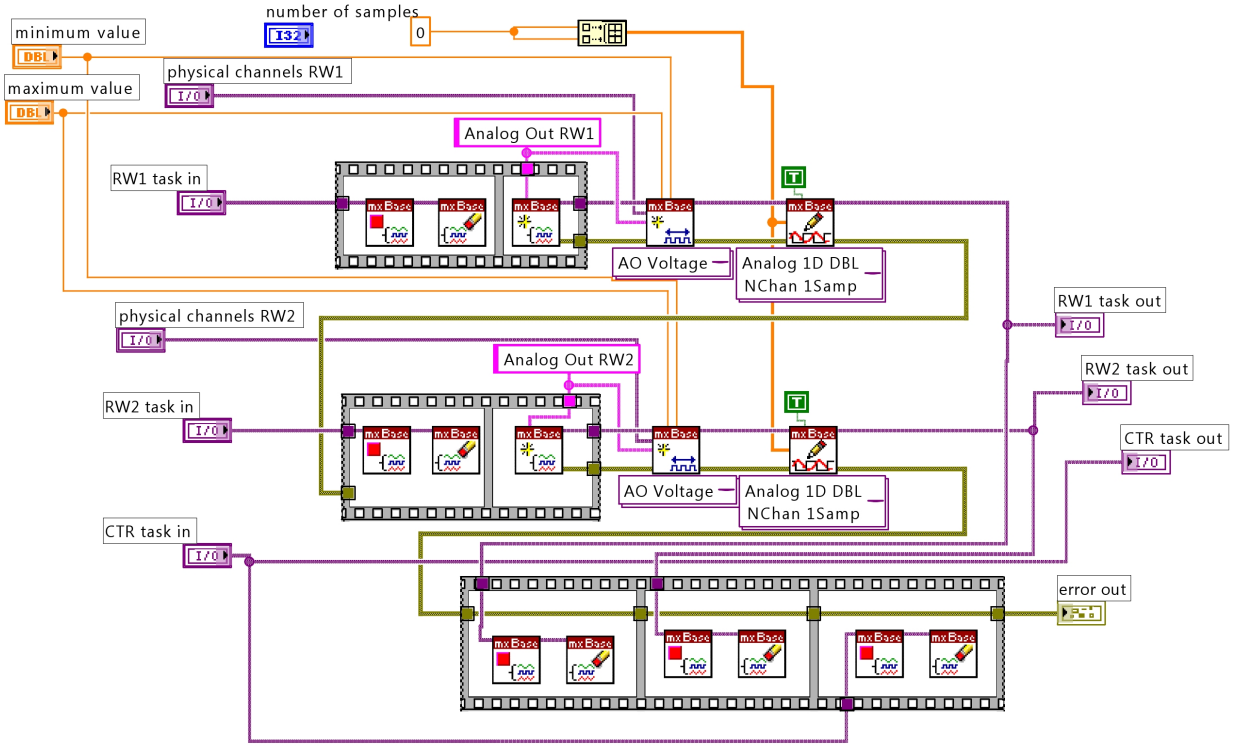

Figure A.2 VI called RWOff used to turn off the Rotating Wall and clear the tasks from memory. Accepts the outputs from RWStart.